Applied Physics A (2020) 126:895
https://doi.org/10.1007/s00339-020-03690-4

Applied Physics A
Materials Science & Processing

Check for updates

$YBa_2Cu_3O_{7-\delta}$ films prepared by pulsed laser deposition in O_2/Ar mixture atmosphere

X. H. Dai[1,2,3] · J. M. Song[1,4] · L. Zhao[1,3] · Y. L. Wang[1,3] · H. D. Zhao[2] · B. T. Liu[1]

Received: 3 December 2019 / Accepted: 27 May 2020 / Published online: 27 October 2020
© Springer-Verlag GmbH Germany, part of Springer Nature 2020

Abstract
The $YBa_2Cu_3O_{7-\delta}$(YBCO) superconducting films were fabricated epitaxially on STO(00 l) substrates by pulsed laser deposition method (PLD) in different O_2/Ar mixture atmospheres. The surface morphology of the YBCO film is strongly dependent on the O_2/Ar ratio of the ambient atmosphere. The surface particle density decreases and the particle size increases with the O_2/Ar ratio decreasing. The lattice parameters and the superconducting transition temperature (T_{c0}) are almost independent on the O_2/Ar ratio and are about the same as 1.168 nm and 90 K, respectively, which can be ascribed to the annealing process in 1 atm O_2 for all the YBCO samples. Based on the above results, in O_2/Ar ratio of 25:75 atmosphere, YBCO:$LaAlO_3$ superconducting composite films with good performance were prepared by co-deposition of PLD with magnetron sputtering method. The experimental results provide a way to control the surface morphology of the YBCO films deposited by PLD method and provide valuable reference for the preparation of YBCO composite thin films by co-deposition of PLD with magnetron sputtering method in Ar/O_2 mixture atmosphere.

Keywords PLD · O_2/Ar mixture atmosphere · YBCO film · Surface morphology · Superconducting transition temperature

1 Introduction

$YBa_2Cu_3O_{7-\delta}$ (YBCO) superconducting films have been the most intensively investigated due to not only the basic physics but also its application background [1–4]. YBCO-based perovskite structure multifunctional heterostructures, such as ferroelectric/superconductor, ferromagnetic/superconductor, colossal magnetoresistance/superconductor, have attracted widespread attention for the potential novel devices [5–10]. Different methods have been used to prepare YBCO thin films, such as metal–organic chemical vapor deposition (MOCVD) [1], metal organic deposition (MOD) [11], pulsed laser deposition (PLD) [4–10], chemical solution deposition (CSD) [12]. Among various techniques, PLD technique has been regarded as one of the most promising methods in preparing multi-component films with precise control of stoichiometry, reproducibility, and simplicity. However, boulders or droplets composed of spherical particles (0.1 ~ 1 μm diameter) and the surface outgrowths composed of misoriented and/or off-stoichiometric crystallites are often observed on the surface of YBCO films [13]. The surface particles seriously impacts the application of the superconducting films on multilayered structures, in particular in electronic devices of diodes and transistors [14–16]. Various attempts have been made to solve this problem, such as laser deposition parameters optimization [17–19], ablation plume processing [20, 21], off-axis laser deposition [22, 23], and the target preparation and modification [24, 25]. However, it is found that the above methods are not very efficient, or even introduce some drawbacks. For example, the region of the optimized deposition parameters is too narrow to find, and small fluctuations may influence the surface quality of the film [17]. The off-axis method in which the substrate has less chance to receive particles may greatly reduce the deposition rate of the film [22]. And the target

✉ B. T. Liu
btliu@hbu.cn

1 College of Physics Science and Technology, Hebei University, Baoding 071002, China

2 College of Electronic and Information Engineering, Hebei University of Technology, Tianjin 300401, China

3 Key Laboratory of High-Precision Computation and Application of Quantum Field Theory of Hebei Province, Baoding, China

4 College of Science, Agriculture University of Hebei, Baoding 071001, China

modification method increases the complexity and technical difficulty of the preparation process [24].

In our experiments, Ar was introduced during fabricating YBCO film by PLD method and the impacts of O_2/Ar ratio on the crystalline quality, surface morphology and transport properties of the YBCO films are systematically studied. The effect of in-situ annealing procedure in 1 atm O_2 on the lattice parameter and transport properties of the YBCO film is discussed. In O_2/Ar ratio of 25:75 atmosphere, YBCO:$LaAlO_3$ superconducting composite films with good performance were prepared successfully by co-deposition of PLD with magnetron sputtering method.

2 Experimental details

The YBCO films with thickness of ~ 100 nm were deposited on 5 mm × 5 mm × 0.5 mm (001)-oriented $SrTiO_3$(STO) substrates by PLD method with a KrF UV excimer laser (248 nm, Coherent) at the base pressure of 1.0×10^{-4} Pa. The distance between the target and substrate was 45 mm. The power density and frequency of the laser were 2.0 J/cm^2 and 2 Hz, respectively. The O_2/Ar mixture atmosphere with the mass flow rate ratio of 100:0, 75:25, 25:75 was set by adjusting the individual gas flows regulated by two calibrated mass flow controllers. The deposition pressure of the O_2/Ar gas mixture was maintained at 15 Pa monitored with a resistance vacuum gauge through adjusting the gate valve. The substrate temperature was kept at 795 ℃ during the deposition process. After the deposition process, oxygen was input into the chamber to reach 1.0×10^5 Pa before the films were cooled from 795 to 520 ℃ at the rate of 10 ℃/min. For the full oxidation of the YBCO films, the temperature was maintained at 520 ℃ for 30 min. The samples were then cooled down to room temperature at the rate of 5 ℃/min. The YBCO films with the same thickness of ~ 100 nm were gained by varying the deposition time from 8 to 12 min when deposited in mixture atmospheres from O_2/Ar ratio of 100:0 to 25:75. To express concisely, hereafter we use S1, S2 and S3 to denote YBCO films deposited in different O_2/Ar ratio of 100:0, 75:25, 25:75, respectively. The surface morphology of the film was studied by scanning electron micrography (SEM) (FEI Nova NanoSEM450). The phase and crystallinity of the YBCO films were characterized by X-ray diffraction (XRD) technique using a Bruker D-8 X-ray diffractometer. The superconducting transport properties of $YBa_2Cu_3O_{7-\delta}$ films were characterized using a physical property measurement system (Quantum design, PPMS-9 T), in which high-purity iridium metal was used as the contact electrodes on YBCO films.

3 Results and discussions

XRD patterns of YBCO films deposited on $SrTiO_3$ substrates in O_2/Ar mixture atmospheres are shown in Fig. 1. From which, it can be seen that besides the substrate peaks, only (00 *l*) diffraction peaks of the YBCO film can be seen for all samples, indicating all the films are highly *c*-axis oriented. Figure 1d presents a typical phi-scan pattern of (014) Bragg peak of the YBCO film, indicative of the epitaxial growth of the YBCO film on STO (001) substrates. Within the measurement error of our X-ray diffraction data, the calculated *c*-axis lattice parameters are almost the same as 1.168 nm for S1 ~ S3 samples [26]. It is reported that the in-situ annealing process in 1 atm O_2 is crucial for the oxidation and the oxygen content of S1 ~ S3 samples in spite of the deposition ambient gas. During the oxygen annealing process, surface chemical adsorption and diffusion of oxygen into the interior of the YBCO films occur [27–29].

The surface particles of S1 ~ S3 samples were identified and counted from scanning electron micrographs (SEM), as shown in Fig. 2a–c. It can be seen that there is a big difference in surface morphology (particle numbers and sizes) for S1 ~ S3. As for S1, the surface particles are distributed densely and uniformly, much smaller particles with the density of 2.0×10^8/cm^2 and mean size of 0.25 μm are presented on the film surface (shown in Fig. 2a), which is the same magnitude as the typical reported densities and sizes [30]. However, in argon diluted oxygen atmosphere (for S2 and S3), less and larger particles are exhibited on the film surface

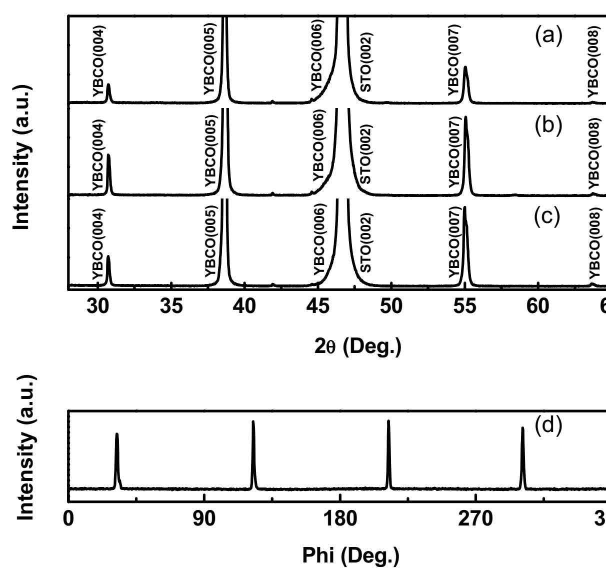

Fig. 1 XRD patterns of YBCO samples deposited in mixture atmosphere of different O_2/Ar ratio **a** 100:0 (S1), **b** 75:25 (S2), **c** 25:75 (S3), respectively. **d** Typical phi-scan pattern of (014) Bragg peak of the YBCO film

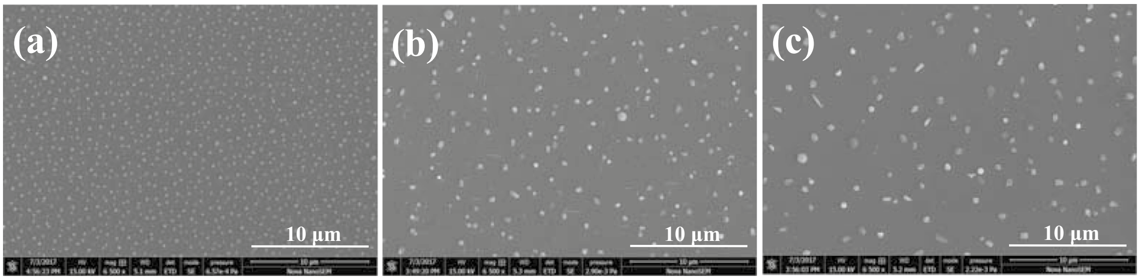

Fig. 2 Surface morphology identified by scanning electron micrographs (SEM) of YBCO samples deposited in mixture atmosphere of different O_2/Ar ratio **a** 100:0 (S1), **b** 75:25 (S2), **c** 25:75 (S3), respectively

(shown in Fig. 2b, c), accompanied with irregular particles, such as needle shaped grains, presented on the film surfaces [31]. The EDX spectra of the surface particles and the matrix around the particles have been measured. The results show that the surface particles are *Y*- and Ba-deficient Cu–O particles. It should be mentioned that the shape and color of the visible plume during the deposition is significantly different for S1 ~ S3 samples. For S1, the plume is more directional and slim with red flame-like of blue color in the center and red color near the boundary. As argon is introduced in the ambient, the plume becomes more diffuse, and the color of plume periphery changes from red to bluish. In our previous study, it is reported that the effective energy transfer and the oscillating stabilization time (OST) produced by the interaction between an ambient atom and a Si atom decide the size distribution of Si nanoparticles prepared in varied mixed atomic ratio (MAR) of the ambient gases by PLD method [32, 33]. The above results indicate that the interaction between the plume and ambient gas may play an important role. It is reported that the typically natural lifetimes of electronic transitions in the plasma plume are of the order of 10^{-8} s [34], and the typical velocities of the ions within the plume are around 10^6 cm/s [35]. Thus, large spatial dimensions of the visible plume can be explained by the interaction between the plume and ambient gas, as well as the absorption of photons from both the laser and the plasma radiation [36]. And the interaction of the ablation plume with ambient background gases is reported not only a complex hydrodynamic phenomenon but also a chemical process [37]. Here in the YBCO deposition process, O_2 and Ar can act as reactive and non-reactive gas, respectively. When the oxygen partial pressure becomes lower with the introduction of the inert Ar gas, the elastic scattering of the plume particles by Ar might be enhanced, so the plume seems more diffuse rather than directional and slim [38]. Meanwhile, the chemically reactive collisions become weak and the reaction rates become slow for the number of O_2 molecules decreases with the introduction of Ar. Therefore the nucleation and growth of the surface clusters become slower, and also do the film deposition rates. The particle distribution on the film surfaces of S1 ~ S3, as well as the film deposition rate obtained based on the film thickness measured by the step profilometer (Bruker, Dektak XT), confirm the above analysis when Ar was introduced to the deposition chamber.

The effect of Ar introduction and the O_2/Ar ratio on the electrical transport properties of the YBCO films were studied. The in-plane resistance (*R*) versus temperature (*T*) relation of the YBCO thin films were presented in Fig. 3 which measured by a standard four-probe electrical measurements. The results show that the resistance value of the YBCO film decreases with the O_2/Ar ratio decreasing, which may be related to the surface particles distribution. It is reported that the surface particles are electrically non-conductive and seriously impacts the application of the superconducting films, so when the surface particles decrease with the O_2/Ar ratio decreasing (shown in Fig. 2), the resistance value of the YBCO film decreases. It can also be seen that the superconducting transition temperature (T_{c0}) is almost the same as ~ 90 K, which is almost independent of the deposition ambient in spite of the significant differences of the surface

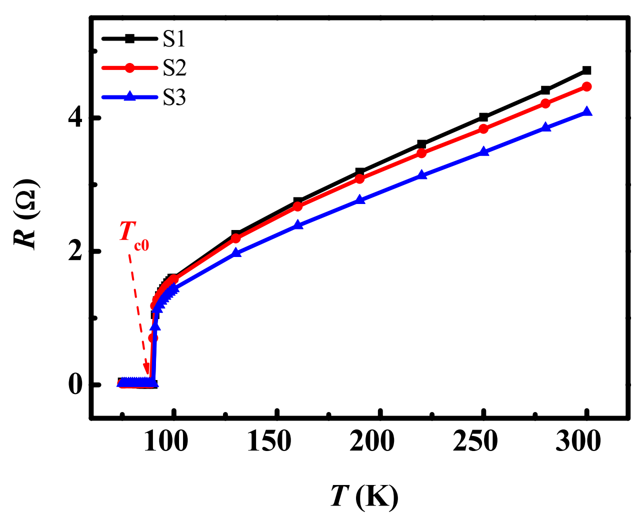

Fig. 3 Dependence of resistance (*R*) on temperature (*T*) for S1 ~ S3 with in-situ annealing in 1 atm O_2

morphology for S1 ~ S3 samples (shown in Fig. 2). It can be concluded that the oxidation and the electrical transport properties were mainly determined by the in-situ annealing process in 1.0×10^5 Pa O_2 atmosphere despite the difference of the deposition ambient gas [27–29].

Based on the above analysis, surface morphology of YBCO thin film can be modified by adjusting the O_2/Ar ratio of the ambient atmosphere and good superconducting performance can be gained through in-situ annealing process in 1.0×10^5 Pa O_2. Coincidentally, the O_2/Ar ratio of 25:75 is commonly used in most of the magnetron sputtering process. It is well known that doping of non-superconducting materials into high temperature superconducting materials can effectively improve the transport properties by introducing artificial pinning centers into the superconductors. Here, the $LaAlO_3$:$YBa_2Cu_3O_{7-\delta}$ superconducting films with thickness of ~ 100 nm were successfully prepared in O_2/Ar ratio of 25:75 atmosphere by co-deposition of PLD with magnetron sputtering method. The YBCO film was prepared by pulsed laser deposition method from a single-phase $YBa_2Cu_3O_{7-\delta}$ target and the $LaAlO_3$ film was deposited from a $LaAlO_3$ target by radio frequency sputtering with the corresponding magnetron power of 25 W. The superconducting transition temperature (T_c) and the critical current density (J_c) in magnetic field of $YBa_2Cu_3O_{7-\delta}$:$LaAlO_3$ superconducting materials have been investigated. As can be seen in Figs. 4 and 5, the doping of $LaAlO_3$ have little effect on the T_c of YBCO films and can effectively improve the critical current densities of the YBCO films in magnetic field higher than 1 T at 77 K. From the inset of Fig. 5, it can be seen that the J_c of $YBa_2Cu_3O_{7-\delta}$:$LaAlO_3$ superconducting film decays more slowly than that of YBCO film in magnetic field higher than 1 T, which implying the co-deposition of PLD with magnetron sputtering method is a valuable approach for the preparation of YBCO composite thin films in Ar/O_2 mixture atmosphere.

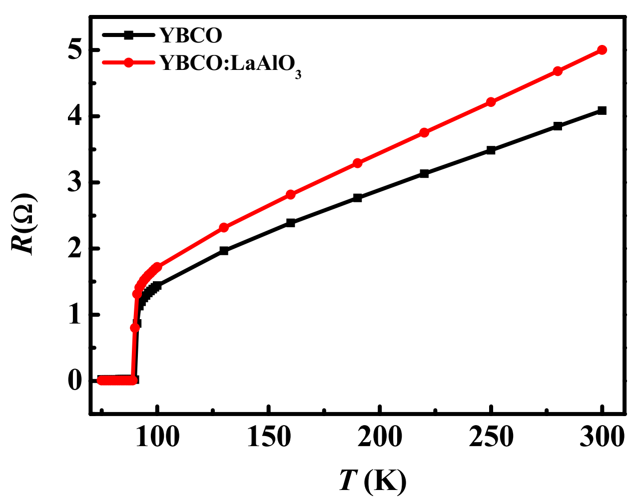

Fig. 4 Dependence of resistance (R) on temperature (T) for YBCO:$LaAlO_3$ composite film compared with YBCO film

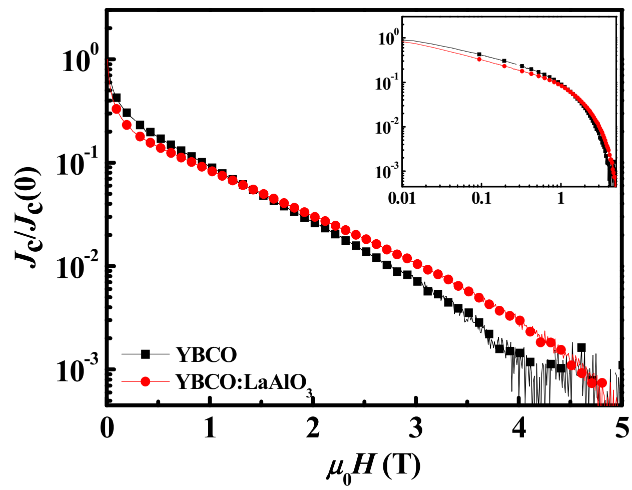

Fig. 5 $J_c/J_c(0)$-H for YBCO:$LaAlO_3$ composite film compared with YBCO film at 77 K. Inset shows $\log J_c/J_c(0)$ vs. $\log H$ plot for magnetic field dependence of $J_c \propto H^{-\alpha}$

4 Conclusions

The introduction of Ar and the O_2/Ar ratio on the crystalline quality, surface morphology and electrical transport properties of the YBCO films deposited by PLD method have been studied intensively. The introduction of Ar has significant effect on the visible laser plume and the surface morphology of the films, but have little effect on the superconducting transition temperature T_c, which can be attributed to the in-situ annealing in 1.0×10^5 Pa O_2. The experimental results provide a way for effectively controlling the surface morphology of the YBCO films deposited by PLD method and provide valuable reference for the preparation of YBCO composite thin films by co-deposition of PLD with magnetron sputtering method in Ar/O_2 mixture atmosphere.

Acknowledgements This work is supported by the National Natural Science Foundation of China (11374086), the Natural Science Foundation of Hebei Province (E2014201188, A2018201168), and the Advanced Talents Incubation Program of Hebei University (521000981323).

References

1. A. Xu, L. Delgado, N. Khatri et al., APL Mater. **2**, 046111 (2014)
2. K. Matsumoto, P. Mele, Supercond. Sci. Technol. **23**, 014001 (2010)
3. S.R. Foltyn, L. Civale, J.L. Macmanus-Driscoll et al., Nat. Mater. **6**, 631 (2007)

4. T. Horide, K. Taguchi, K. Matsumoto et al., Appl. Phys. Lett. **108**, 082601 (2016)
5. D. Springer, S.K. Nair, M. He et al., Phys. Rev. B **93**, 064510 (2016)
6. M. Sharma, K.K. Sharma, R.J. Choudhary et al., J. Appl. Phys. **116**, 233905 (2014)
7. M.J. Zhang, F.X. Hao, C. Zhang et al., Appl. Phys. Lett. **107**, 183508 (2015)
8. F.X. Hao, C. Zhang, X. Liu et al., Appl. Phys. Lett. **109**, 131104 (2016)
9. F.G. Liu, X.K. Lian, J. Hou et al., J. Alloys and Comp. **619**, 505 (2015)
10. H.J. Zhang, X.P. Zhang, J.P. Shi et al., Appl. Phys. Lett. **94**, 092111 (2009)
11. M. Miura, B. Maiorov, S.A. Baily et al., Phys. Rev. B **83**, 184519 (2011)
12. A. Llordés, A. Palau, J. Gázquez et al., Nat. Mater. **11**, 329 (2012)
13. S. Proyer, E. Stangl, M. Borz et al., Physica C **257**, 1–15 (1996)
14. L. Avils F´elix, M. Sirena, L. A. Agüero Guzm´an, et al. Nanotechnology, **23**:495715 (2012).
15. S. Yoshihisa, F. Tokuumi, IEEE Trans. Appl. Supercond. **13**, 591 (2003)
16. M. I. Faley, S. B. Mi, A. Petraru., Appl. Phys. Lett. **89,** 1(2006).
17. X.D. Wu, A. Inam, T. Venkatesan et al., Appl. Phys. Lett. **52**, 754 (1988)
18. H.S. Kim, H.S. Kwok, Appl. Phys. Lett. **61**, 2234 (1992)
19. M. Brănescu, A. Vailionis, J. Huh et al., Appl. Surf. Sci. **253**, 8179 (2007)
20. M.D. Strikovsky, E.B. Klyuenkov, S.V. Gapanov et al., Appl. Phys. Lett. **63**, 1146 (1993)
21. E.V. Pechen, A.V. Varlashkin, S.I. Krasnosvobodtsev et al., Appl. Phys. Lett. **66**(17), 2292 (1995)
22. B. Holzapfel, B. Roas, L. Schultz et al., Appl. Phys. Lett. **61**, 3178 (1992)
23. V. Boffa, T. Petrisor, L. Ciontea et al., Physica C **276**, 218 (1997)
24. Y. S. Jeong, S. Y. Lee, H. K. Jang, et al. Appl. Surf. Sci. **109/110**, 424 (1997).
25. C. Doughty, A.T. Findikoglu, T. Venkatesan, Appl. Phys. Lett. **66**(10), 1276 (1995)
26. R. Zhao, W.W. Li, J.H. Lee et al., Adv. Funct. Mater. **24**, 5240 (2014)
27. R.E. Sudhakar, T. Rajasekharan, Physica C **279**, 56 (1997)
28. H.Y. Zhai, Z.H. Zhang, W.K. Chu, Appl. Phys. Lett. **78**(5), 29 (2001)
29. D. Shi, K. Zhang, D.W. Capone II, J. Appl. Phys. **64**(4), 1995 (1988)
30. T.I. Selinder, U. Helmersson, Z. Han et al., Physica C **202**, 69 (1992)
31. A. Catana, J.G. Bednorz, Ch Gerber et al., Appl. Phys. Lett. **63**(4), 26 (1993)
32. Y.L. Wang, Z.C. Deng, G.S. Fu et al., Thin Solid Films **515**, 1897 (2006)
33. Y.L. Wang, L.Z. Chu, Y.L. Li et al., Micro & Nano Letters **4**(1), 39 (2009)
34. C. Girault, D. Damiani, J. Aubreton et al., Appl. Phys. Lett. **54**, 2035 (1989)
35. J.P. Zheng, Z.Q. Huang, D.T. Shaw et al., Appl. Phys. Lett. **54**, 280 (1988)
36. S. Proyer, E. Stangl, Appl. Phys. A. **60**, 573 (1995)
37. X.Y. Chen, S.B. Xiong, Z.S. Sha et al., Appl. Surf. Sci. **115**, 279 (1997)
38. M.S. Tsai, S.C. Sun, T.Y. Tseng, J. Appl. Phys. **82**(7), 3482 (1997)

Publisher's Note Springer Nature remains neutral with regard to jurisdictional claims in published maps and institutional affiliations.